

Pattern of indirect excitons in van der Waals heterostructure

Zhiwen Zhou,¹ L. H. Fowler-Gerace,¹ W. J. Brunner,¹ E. A. Szwed,¹ and L. V. Butov¹

¹*Department of Physics, University of California San Diego, La Jolla, CA 92093, USA*

(Dated: February 24, 2026)

We studied photoluminescence of spatially indirect excitons (IXs) in a MoSe₂/WSe₂ van der Waals heterostructure. We observed a quasi-periodic triangular pattern of IXs with the characteristic wavelength of the pattern $\sim 2.6 \mu\text{m}$.

A spatial modulation of exciton luminescence is a basic phenomenon explored in various excitonic systems. Indirect excitons (IXs), also known as interlayer excitons, are composed of electrons and holes in separated layers [1]. Due to the layer separation, IX lifetimes are significantly longer than lifetimes of regular spatially direct excitons (DX) [2]. The long lifetime allows IXs to cool to low temperatures [1] and the efficient IX thermalization facilitates a spatial modulation of IX luminescence.

Various mechanisms can be responsible for modulations in excitonic systems. For instance, a periodic modulation of exciton luminescence can be caused by Turing instability driven by stimulated kinetics of exciton formation due to quantum degeneracy [3, 4]. Studies of IXs in GaAs heterostructures led to the observation of the exciton ring modulation [5–7], which is caused by this instability [3]. The wavelength of this instability is controlled by density [3] and varies in the range $\sim 9 - 40 \mu\text{m}$ in the experiments [5–7]. A triangular pattern of IXs due to this instability was predicted for electron-hole systems [4].

A modulation of exciton luminescence can also emerge due to attractive interaction. For instance, a modulation due to attractive interaction was observed in cold atoms [8].

Van der Waals heterostructures allow exploring new mechanisms for modulations of exciton luminescence. Twisting between the layers in a van der Waals heterostructure can lead to the IX modulation caused by moiré [9–23] and super moiré [24–26] lattices. The modulation period is given by the period of the moiré superlattice and is typically in the range from few nm to few hundred nm [9–26].

In this work, we present the observation of a quasi-periodic triangular pattern of IXs with the characteristic wavelength of the pattern $\sim 2.6 \mu\text{m}$ in a MoSe₂/WSe₂ van der Waals heterostructure. We compare the observed pattern with various modulation mechanisms.

Experiments. We study IXs in a MoSe₂/WSe₂ heterostructure (Fig. 1a) where adjacent MoSe₂ monolayer and WSe₂ monolayer form the separated electron and hole layers for IXs [27]. The heterostructure was assembled as described in Ref. [28] where the same heterostructure was used for IX transport studies. The dry-transfer peel technique [29] was used. The MoSe₂ and

WSe₂ monolayers are encapsulated by hBN (Fig. 1a,b) with $\sim 40\text{-nm}$ -thick bottom hBN and $\sim 30\text{-nm}$ -thick top hBN covering the entire MoSe₂ and WSe₂ areas. The long WSe₂ and MoSe₂ edges were used for a rotational alignment between the WSe₂ and MoSe₂ monolayers. The twist angle between these monolayers $\delta\theta = 1.1^\circ$ corresponding to the moiré superlattice period $b \sim a/\delta\theta \sim 17 \text{ nm}$ (a is the lattice period) agrees with the angle between the long WSe₂ and MoSe₂ edges in the heterostructure [28]. The moiré potentials can be affected by atomic reconstruction [30–32] and disorder and may vary over the heterostructure area. The IX g -factor ~ -16 in the heterostructure corresponds to H stacking [16, 33]. The mechanically exfoliated layers of the heterostructure were stacked on graphite substrate pressed onto Si/SiO₂ substrate.

Excitons were generated by a cw Ti:Sapphire laser with the excitation energy $E_{\text{ex}} = 1.689 \text{ eV}$ resonant to DX in WSe₂ heterostructure layer. The laser excitation was focused to $\sim 2 \mu\text{m}$ spot. The IX photoluminescence (PL) was selected by a filter $E \lesssim 1.4 \text{ eV}$ and images of IX PL intensity were measured using a liquid-nitrogen-cooled CCD with a spatial resolution $0.8 \mu\text{m}$. The studied sample is a unique sample, which shows the long-range IX transport [28] and the long-range IX mediated spin transport [34]. We hesitate risking this unique sample by performing the measurements, which may compromise the sample quality. Therefore, we limit the measurements by the optical measurements outlined in this work. The experiments were performed in a variable-temperature 4He cryostat. The IX pattern reported in the paper was reproducible after many cycles of cooling down to $\sim 2 \text{ K}$ and warming up to room temperature.

The IX PL images (Fig. 1c) show a spatial modulation of IX PL intensity $I(x, y)$. This modulation is more pronounced in Fig. 1e showing $-\Delta I = -(\partial^2 I/\partial x^2 + \partial^2 I/\partial y^2)$. The cyan dots in Figs. 1d and 1f indicate the positions of local maxima in $-\Delta I(x, y)$. These maxima form a quasi-periodic IX pattern.

The characteristics of this IX pattern are presented in Fig. 2. The average distance between the local maxima in $-\Delta I(x, y)$ is $\sim 2.6 \mu\text{m}$ (Fig. 2a). This lengthscale corresponds to the broad peak in the Fourier transform of $-\Delta I(x, y)$ along the line connecting the local maxima (Fig. 2b). The characteristic angle between the lines connecting the local maxima in $-\Delta I(x, y)$ is $\sim 60^\circ$ (Fig. 2c).

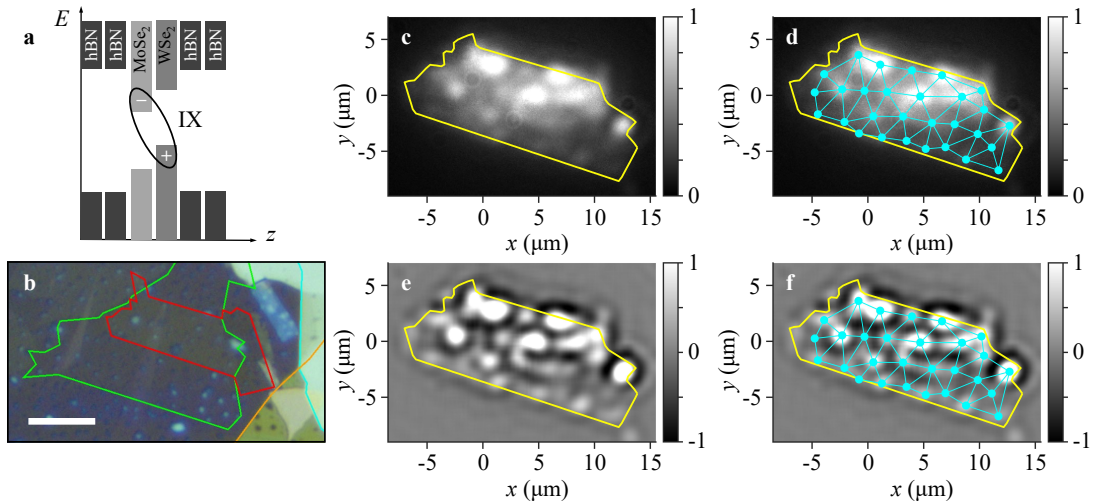


FIG. 1: IX pattern. (a) Schematic energy-band diagram for the heterostructure. The oval indicates an indirect exciton (IX) composed of an electron (-) and a hole (+). (b) A microscope image showing the layers of the heterostructure. Scale bar is $10 \mu\text{m}$. The red, green, cyan, and orange lines indicate the boundaries of MoSe_2 and WSe_2 monolayers and bottom and top hBN layers, respectively. (c,d) An image of IX PL intensity $I(x, y)$. (e,f) The pattern of $-\Delta I(x, y)$ highlighting the spatial modulation of $I(x, y)$. The cyan dots in (d,f) indicate the positions of local maxima in $-\Delta I(x, y)$. These maxima form a quasi-periodic triangular pattern. The yellow line in (c-f) shows the boundary of the $\text{MoSe}_2/\text{WSe}_2$ heterostructure. The laser excitation power $P_{\text{ex}} = 0.2 \text{ mW}$, temperature $T = 1.7 \text{ K}$. The $\sim 2 \mu\text{m}$ laser excitation spot is centered at $(1.2, 3.2)$.

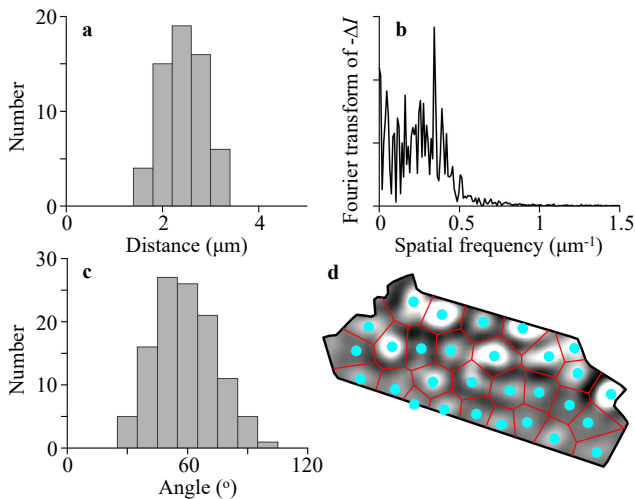


FIG. 2: Characteristics of IX pattern. (a) A histogram of the distances between the local maxima in $-\Delta I(x, y)$. The characteristic wavelength $\lambda \sim 2.6 \mu\text{m}$. (b) The Fourier transform of $-\Delta I(x, y)$ along the line connecting the local maxima. The broad peak on a noise background corresponds to a quasi-periodic modulation with the λ lengthscale. (c) A histogram of the angles between the lines connecting the local maxima in $-\Delta I(x, y)$. The characteristic angle is $\sim 60^\circ$. (d) The Voronoi diagram for the local maxima in $-\Delta I(x, y)$ shown by cyan dots. The Voronoi cells are marked by red lines. The average coordination number for the full Voronoi cells, unbroken by the heterostructure edges, is six. The data correspond to the IX pattern in Fig. 1. These data characterize the IX pattern as a distorted triangular pattern.

Figure 2d shows the Voronoi tessellation for the local maxima in $-\Delta I(x, y)$. For the Voronoi tessellation, the number of neighbors that share a common edge gives the coordination number. The Voronoi tessellation shows that for nine full Voronoi cells, unbroken by the heterostructure edges, seven have six neighbors, one five neighbors, and one seven neighbors. The average coordination number is six. These data characterize the IX pattern as a distorted triangular pattern with the modulation wavelength $\lambda \sim 2.6 \mu\text{m}$.

The density and temperature dependence of the IX modulation are presented in Figs. 3 and 4 showing the $I(x)$ and $-\Delta I(x)$ profiles along x . The IX PL signal is integrated within $1 \mu\text{m}$ in y direction. The IX transport from the laser excitation spot enhances with increasing laser excitation power P_{ex} for $P_{\text{ex}} \lesssim 0.2 \text{ mW}$ and reduces with increasing P_{ex} for higher P_{ex} that is seen from the variation of the IX decay distance in Fig. 3a. The IX long-range transport vanishes at temperatures above $\sim 10 \text{ K}$ (Fig. 4a). These variations of IX transport with density and temperature were studied in Ref. [28]. Figures 3 and 4 show that the quasi-periodic IX modulation is observed along the entire IX signal extension for all the densities and temperatures and the modulation wavelength essentially does not change with density or temperature.

The efficient IX transport with IXs travelling from the laser excitation spot ($x = 0$) to the heterostructure edge ($x \sim 10 \mu\text{m}$) with essentially no decay is observed at intermediate densities in Fig. 3 and low temperatures in Fig. 4. This efficient IX transport, studied in Ref. [28],

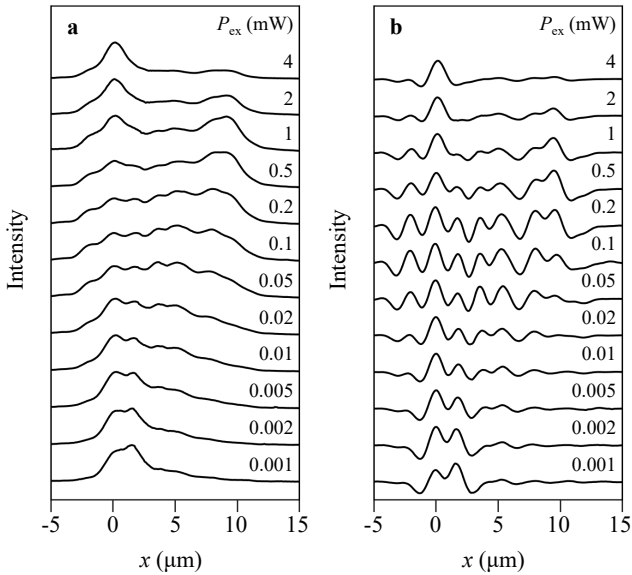


FIG. 3: Density dependence. (a,b) Normalized profiles $I(x)$ (a) and $-\Delta I(x)$ (b) of IX PL showing the quasi-periodic modulation of $I(x)$ (a) and $-\Delta I(x)$ (b) along x for different excitation densities P_{ex} . The $\sim 2 \mu\text{m}$ laser excitation spot is centered at $x = 0, y = 0$. $T = 3.5 \text{ K}$.

coexists with the quasi-periodic IX modulation (Figs. 3 and 4).

Discussions. The origin of the observed exciton quasi-periodic triangular pattern with the characteristic wavelength $\sim 2.6 \mu\text{m}$ in $\text{MoSe}_2/\text{WSe}_2$ van der Waals heterostructure is discussed below. A periodic modulation of exciton luminescence caused by Turing instability (modulational instability) driven by stimulated kinetics of exciton formation due to quantum degeneracy, outlined in the introduction, vanishes with increasing temperature and the modulation wavelength changes with density [3–7]. However, the IX modulation is observed along the IX signal extension for all the temperatures (Fig. 4) and the IX modulation wavelength essentially does not change with the density (Fig. 3). Therefore, the Turing instability is an unlikely mechanism for the observed IX pattern.

IXs are dipoles oriented perpendicular to the heterostructure layers and interaction between them is dominated by the dipolar repulsion as shown by the studies of IX interaction both in GaAs heterostructures [35–45] and in van der Waals heterostructures [27, 28, 46–48]. Therefore, the attractive-interaction mechanism of instability [8] is also an unlikely mechanism for the observed IX pattern.

The characteristic wavelength of the pattern, $\lambda \sim 2.6 \mu\text{m}$, is significantly larger than the period of the moiré superlattice caused by twisting between the MoSe_2 and

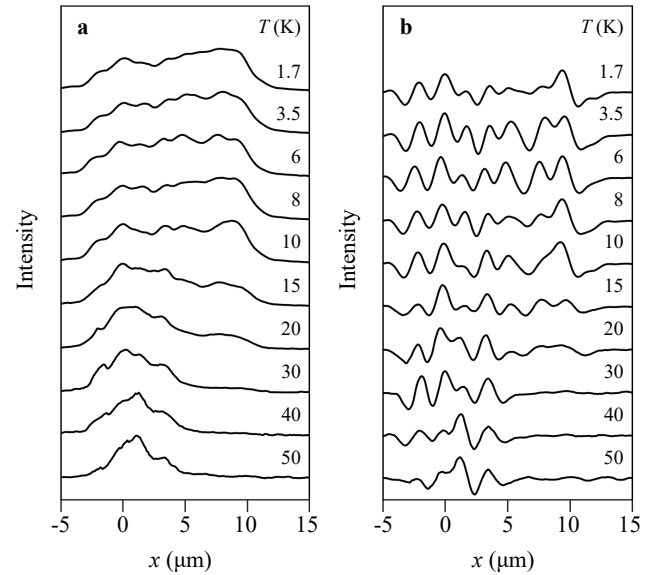


FIG. 4: Temperature dependence. (a,b) Normalized profiles $I(x)$ (a) and $-\Delta I(x)$ (b) of IX PL showing the quasi-periodic modulation of $I(x)$ (a) and $-\Delta I(x)$ (b) along x for different temperatures T . The $\sim 2 \mu\text{m}$ laser excitation spot is centered at $x = 0, y = 0$. $P_{\text{ex}} = 0.2 \text{ mW}$.

WSe_2 layers $b \sim a/\delta\theta \sim 17 \text{ nm}$ [28]. Therefore, the moiré superlattice is also an unlikely mechanism for the observed IX pattern.

A quasi-periodic pattern with a micrometer-scale characteristic wavelength can emerge due to wrinkling in the heterostructure. For a thin film coupled to elastic substrate, an in-plane stress can cause an elastic instability with a periodic pattern of wrinkles [49–51]. In particular, this instability is studied for 2D materials [52–57]. The optimum wrinkling wavelength λ_w is given by the film thickness t and the plane strain moduli of the film \bar{E}_f and the substrate \bar{E}_s : $\lambda_w \sim 2\pi t (\bar{E}_f/3\bar{E}_s)^{1/3}$, where $\bar{E} = E/(1-\nu^2)$, E is the material Young’s modulus and ν the Poisson’s ratio. A stress in the structure can appear due to fabrication and packaging. The wavelength λ_w characterizes the wrinkles for a broad range of the stress [49–51]. Rough estimates for the heterostructure give λ_w on a micrometer scale. For instance, for the 70-nm hBN film coupled to graphite substrate, $E_f \sim 800 \text{ GPa}$, $E_s \sim 20 \text{ GPa}$, and $\nu_{f,s} \sim 0.2$, this rough estimate gives $\lambda_w \sim 1 \mu\text{m}$. The micrometer scale is comparable to the IX modulation wavelength $\lambda \sim 2.6 \mu\text{m}$, indicating that the wrinkling mechanism is qualitatively consistent with the IX modulation pattern.

In summary, we found a quasi-periodic triangular pattern of IXs with the characteristic wavelength of the pattern $\sim 2.6 \mu\text{m}$ in a $\text{MoSe}_2/\text{WSe}_2$ van der Waals heterostructure. We compared the observed pattern with various modulation mechanisms.

Acknowledgements. We thank M.M. Fogler, A.H. MacDonald, and D.E. Parker for discussions and A.K. Geim for teaching us manufacturing van der Waals heterostructures. The experiments were supported by the Department of Energy, Office of Basic Energy Sciences, under award DE-FG02-07ER46449. The heterostructure manufacturing was supported by NSF Grant 1905478. The data analysis was supported by NSF Grant 2516006.

References

-
- [1] Y.E. Lozovik, V.I. Yudson, A new mechanism for superconductivity: pairing between spatially separated electrons and holes, *Sov. Phys. JETP* **44**, 389 (1976).
- [2] A. Zrenner, P. Leeb, J. Schäfler, G. Böhm, G. Weimann, J.M. Worlock, L.T. Florez, J.P. Harbison, Indirect excitons in coupled quantum well structures, *Surf. Sci.* **263**, 496 (1992).
- [3] L.S. Levitov, B.D. Simons, L.V. Butov, Pattern Formation as a Signature of Quantum Degeneracy in a Cold Exciton System, *Phys. Rev. Lett.* **94**, 176404 (2005).
- [4] L.S. Levitov, B.D. Simons, L.V. Butov, Pattern formation in exciton system near quantum degeneracy, *Solid State Commun.* **134**, 51 (2005).
- [5] L.V. Butov, A.C. Gossard, D.S. Chemla, Macroscopically ordered state in an exciton system, *Nature* **418**, 751 (2002).
- [6] L.V. Butov, L.S. Levitov, A.V. Mintsev, B.D. Simons, A.C. Gossard, D.S. Chemla, Formation Mechanism and Low-Temperature Instability of Exciton Rings, *Phys. Rev. Lett.* **92**, 117404 (2004).
- [7] Sen Yang, L.V. Butov, B.D. Simons, K.L. Campman, A.C. Gossard, Fluctuation and commensurability effect of exciton density wave, *Phys. Rev. B* **91**, 245302 (2015).
- [8] Kevin E. Strecker, Guthrie B. Partridge, Andrew G. Truscott, Randall G. Hulet, Formation and propagation of matter-wave soliton trains, *Nature* **417**, 150 (2002).
- [9] Fengcheng Wu, Timothy Lovorn, A.H. MacDonald, Theory of optical absorption by interlayer excitons in transition metal dichalcogenide heterobilayers, *Phys. Rev. B* **97**, 035306 (2018).
- [10] Hongyi Yu, Gui-Bin Liu, Wang Yao, Brightened spin-triplet interlayer excitons and optical selection rules in van der Waals heterobilayers, *2D Mater.* **5**, 035021 (2018).
- [11] Fengcheng Wu, Timothy Lovorn, A.H. MacDonald, Topological Exciton Bands in Moiré Heterojunctions, *Phys. Rev. Lett.* **118**, 147401 (2017).
- [12] Hongyi Yu, Gui-Bin Liu, Jianju Tang, Xiaodong Xu, Wang Yao, Moiré excitons: From programmable quantum emitter arrays to spin-orbit-coupled artificial lattices, *Sci. Adv.* **3**, e1701696 (2017).
- [13] Chendong Zhang, Chih-Piao Chuu, Xibiao Ren, Ming-Yang Li, Lain-Jong Li, Chuanhong Jin, Mei-Yin Chou, Chih-Kang Shih, Interlayer couplings, Moiré patterns, and 2D electronic superlattices in MoS₂/WSe₂ hetero-bilayers, *Sci. Adv.* **3**, e1601459 (2017).
- [14] Nan Zhang, Alessandro Surrente, Michał Baranowski, Duncan K. Maude, Patricia Gant, Andres Castellanos-Gomez, Paulina Plochocka, Moiré Intralayer Excitons in a MoSe₂/MoS₂ Heterostructure, *Nano Lett.* **18**, 7651 (2018).
- [15] Alberto Ciarrocchi, Dmitrii Unuchek, Ahmet Avsar, Kenji Watanabe, Takashi Taniguchi, Andras Kis, Polarization switching and electrical control of interlayer excitons in two-dimensional van der Waals heterostructures, *Nat. Photonics* **13**, 131 (2019).
- [16] Kyle L. Seyler, Pasqual Rivera, Hongyi Yu, Nathan P. Wilson, Essance L. Ray, David G. Mandrus, Jiaqiang Yan, Wang Yao, Xiaodong Xu, Signatures of moiré-trapped valley excitons in MoSe₂/WSe₂ heterobilayers, *Nature* **567**, 66 (2019).
- [17] Kha Tran, Galan Moody, Fengcheng Wu, Xiaobo Lu, Junho Choi, Kyoungwan Kim, Amritesh Rai, Daniel A. Sanchez, Jiamin Quan, Akshay Singh, Jacob Embley, André Zepeda, Marshall Campbell, Travis Autry, Takashi Taniguchi, Kenji Watanabe, Nanshu Lu, Sanjay K. Banerjee, Kevin L. Silverman, Suenne Kim, Emanuel Tutuc, Li Yang, Allan H. MacDonald, Xiaoqin Li, Evidence for moiré excitons in van der Waals heterostructures, *Nature* **567**, 71 (2019).
- [18] Chenhao Jin, Emma C. Regan, Aiming Yan, M. Iqbal Bakti Utama, Danqing Wang, Sihan Zhao, Ying Qin, Sijie Yang, Zhiren Zheng, Shenyang Shi, Kenji Watanabe, Takashi Taniguchi, Sefaattin Tongay, Alex Zettl, Feng Wang, Observation of moiré excitons in WSe₂/WS₂ heterostructure superlattices, *Nature* **567**, 76 (2019).
- [19] Evgeny M. Alexeev, David A. Ruiz-Tijerina, Mark Danovich, Matthew J. Hamer, Daniel J. Terry, Pramoda K. Nayak, Seongjoon Ahn, Sangyeon Pak, Juwon Lee, Jung Inn Sohn, Maciej R. Molas, Maciej Koperski, Kenji Watanabe, Takashi Taniguchi, Kostya S. Novoselov, Roman V. Gorbachev, Hyeon Suk Shin, Vladimir I. Fal'ko, Alexander I. Tartakovskii, Resonantly hybridized excitons in moiré superlattices in van der Waals heterostructures, *Nature* **567**, 81 (2019).
- [20] Chenhao Jin, Emma C. Regan, Danqing Wang, M. Iqbal Bakti Utama, Chan-Shan Yang, Jeffrey Cain, Ying Qin, Yuxia Shen, Zhiren Zheng, Kenji Watanabe, Takashi Taniguchi, Sefaattin Tongay, Alex Zettl, Feng Wang, Identification of spin, valley and moiré quasi-angular momentum of interlayer excitons, *Nat. Phys.* **15**, 1140 (2019).
- [21] Yuya Shimazaki, Ido Schwartz, Kenji Watanabe, Takashi Taniguchi, Martin Kroner, Ataç Imamoğlu, Strongly correlated electrons and hybrid excitons in a moiré heterostructure, *Nature* **580**, 472 (2020).
- [22] Nathan P. Wilson, Wang Yao, Jie Shan, Xiaodong Xu, Excitons and emergent quantum phenomena in stacked 2D semiconductors, *Nature* **599**, 383 (2021).
- [23] Jie Gu, Liguang Ma, Song Liu, Kenji Watanabe, Takashi Taniguchi, James C. Hone, Jie Shan, Kin Fai Mak, Dipolar excitonic insulator in a moiré lattice, *Nat. Phys.* **18**, 395 (2022).
- [24] Zihao Wang, Yi Bo Wang, J. Yin, E. Tóvári, Y. Yang, L. Lin, M. Holwill, J. Birkbeck, D.J. Perello, Shuigang Xu, J. Zultak, R.V. Gorbachev, A.V. Kretinin, T. Taniguchi, K. Watanabe, S.V. Morozov, M. Andelković, S.P. Milovanović, L. Covaci, F.M. Peeters, A. Mishchenko, A.K. Geim, K.S. Novoselov, Vladimir I. Fal'ko, Angelika Knothe, C.R. Woods, Composite super-moiré lattices in double-aligned graphene heterostructures, *Sci. Adv.* **5**, eaay8897 (2019).
- [25] Li-Qiao Xia, Sergio C. de la Barrera, Aviram Uri, Aaron

- Sharpe, Yves H. Kwan, Ziyang Zhu, Kenji Watanabe, Takashi Taniguchi, David Goldhaber-Gordon, Liang Fu, Trithem Devakul, Pablo Jarillo-Herrero, Topological bands and correlated states in helical trilayer graphene, *Nat. Phys.* **21**, 239 (2025).
- [26] Yonglong Xie, Andrew T. Pierce, Jeong Min Park, Daniel E. Parker, Jie Wang, Patrick Ledwith, Zhuozhen Cai, Kenji Watanabe, Takashi Taniguchi, Eslam Khalaf, Ashvin Vishwanath, Pablo Jarillo-Herrero, Amir Yacoby, Strong interactions and isospin symmetry breaking in a supermoiré lattice, *Science* **389**, 736 (2025).
- [27] Pasqual Rivera, John R. Schaibley, Aaron M. Jones, Jason S. Ross, Sanfeng Wu, Grant Aivazian, Philip Klement, Kyle Seyler, Genevieve Clark, Nirmal J. Ghimire, Jiaqiang Yan, D.G. Mandrus, Wang Yao, Xiaodong Xu, Observation of long-lived interlayer excitons in monolayer MoSe₂-WSe₂ heterostructures, *Nat. Commun.* **6**, 6242 (2015).
- [28] L.H. Fowler-Gerace, Zhiwen Zhou, E.A. Szwed, D.J. Choksy, L.V. Butov, Transport and localization of indirect excitons in a van der Waals heterostructure, *Nat. Photon.* **18**, 823 (2024).
- [29] F. Withers, O. Del Pozo-Zamudio, A. Mishchenko, A.P. Rooney, A. Gholinia, K. Watanabe, T. Taniguchi, S.J. Haigh, A.K. Geim, A.I. Tartakovskii, K.S. Novoselov, Light-emitting diodes by band-structure engineering in van der Waals heterostructures, *Nat. Mater.* **14**, 301 (2015).
- [30] Astrid Weston, Yichao Zou, Vladimir Enaldiev, Alex Summerfield, Nicholas Clark, Viktor Zólyomi, Abigail Graham, Celal Yelgel, Samuel Magorrian, Mingwei Zhou, Johanna Zultak, David Hopkinson, Alexei Barinov, Thomas H. Bointon, Andrey Kretinin, Neil R. Wilson, Peter H. Beton, Vladimir I. Fal'ko, Sarah J. Haigh, Roman Gorbachev, Atomic reconstruction in twisted bilayers of transition metal dichalcogenides, *Nat. Nanotechnol.* **15**, 592 (2020).
- [31] Matthew R. Rosenberger, Hsun-Jen Chuang, Madeleine Phillips, Vladimir P. Oleshko, Kathleen M. McCreary, Saujan V. Sivaram, C. Stephen Hellberg, Berend T. Jonker, Twist Angle-Dependent Atomic Reconstruction and Moiré Patterns in Transition Metal Dichalcogenide Heterostructures, *ACS Nano* **14**, 4550 (2020).
- [32] Shen Zhao, Zhijie Li, Xin Huang, Anna Rupp, Jonas Göser, Iliia A. Vovk, Stanislav Yu. Kruchinin, Kenji Watanabe, Takashi Taniguchi, Ismail Bilgin, Anvar S. Baimuratov, Alexander Högele, Excitons in mesoscopically reconstructed moiré heterostructures, *Nat. Nanotechnol.* **18**, 572 (2023).
- [33] Tomasz Woźniak, Paulo E. Faria Junior, Gotthard Seifert, Andrey Chaves, Jens Kunstmann, Exciton g factors of van der Waals heterostructures from first-principles calculations, *Phys. Rev. B* **101**, 235408 (2020).
- [34] Zhiwen Zhou, E.A. Szwed, D.J. Choksy, L.H. Fowler-Gerace, L.V. Butov, Long-distance decay-less spin transport in indirect excitons in a van der Waals heterostructure, *Nat. Commun.* **15**, 9454 (2024).
- [35] D. Yoshioka, A.H. MacDonald, Double Quantum Well Electron-Hole Systems in Strong Magnetic Fields, *J. Phys. Soc. Jpn.* **59**, 4211 (1990).
- [36] L. V. Butov, A. Zrenner, G. Abstreiter, G. Böhm, G. Weimann, Condensation of Indirect Excitons in Coupled AlAs/GaAs Quantum Wells, *Phys. Rev. Lett.* **73**, 304 (1994).
- [37] X. Zhu, P.B. Littlewood, M.S. Hybertsen, T.M. Rice, Exciton Condensate in Semiconductor Quantum Well Structures, *Phys. Rev. Lett.* **74**, 1633 (1995).
- [38] Yu.E. Lozovik, O.L. Berman, Phase transitions in a system of spatially separated electrons and holes, *J. Exp. Theor. Phys.* **84**, 1027 (1997).
- [39] S. De Palo, F. Rapisarda, G. Senatore, Excitonic Condensation in a Symmetric Electron-Hole Bilayer, *Phys. Rev. Lett.* **88**, 206401 (2002).
- [40] A.L. Ivanov, Quantum diffusion of dipole-oriented indirect excitons in coupled quantum wells, *Europhys. Lett.* **59**, 586 (2002).
- [41] S. Ben-Tabou de Leon, B. Laikhtman, Mott transition, biexciton crossover, and spin ordering in the exciton gas in quantum wells, *Phys. Rev. B* **67**, 235315 (2003).
- [42] C. Schindler, R. Zimmermann, Analysis of the exciton-exciton interaction in semiconductor quantum wells, *Phys. Rev. B* **78**, 045313 (2008).
- [43] B. Laikhtman, R. Rapaport, Exciton correlations in coupled quantum wells and their luminescence blue shift, *Phys. Rev. B* **80**, 195313 (2009).
- [44] R. Maezono, P. López Ríos, T. Ogawa, R.J. Needs, Excitons and biexcitons in symmetric electron-hole bilayers, *Phys. Rev. Lett.* **110**, 216407 (2013).
- [45] M. Remeika, J.R. Leonard, C.J. Dorow, M.M. Fogler, L.V. Butov, M. Hanson, A.C. Gossard, Measurement of exciton correlations using electrostatic lattices, *Phys. Rev. B* **92**, 115311 (2015).
- [46] Philipp Nagler, Gerd Plechinger, Mariana V. Ballottin, Anatolie Mitioglu, Sebastian Meier, Nicola Paradiso, Christoph Strunk, Alexey Chernikov, Peter C.M. Christianen, Christian Schüller, Tobias Korn, Interlayer exciton dynamics in a dichalcogenide monolayer heterostructure, *2D Mater.* **4**, 025112 (2017).
- [47] Malte Kremser, Mauro Brotons-Gisbert, Johannes Knörzer, Janine Gückelhorn, Moritz Meyer, Matteo Barbone, Andreas V. Stier, Brian D. Gerardot, Kai Müller, Jonathan J. Finley, Discrete interactions between a few interlayer excitons trapped at a MoSe₂-WSe₂ heterointerface, *npj 2D Mater. Appl.* **4**, 8 (2020).
- [48] Zhe Sun, Alberto Ciarrocchi, Fedele Tagarelli, Juan Francisco Gonzalez Marin, Kenji Watanabe, Takashi Taniguchi, Andras Kis, Excitonic transport driven by repulsive dipolar interaction in a van der Waals heterostructure, *Nat. Photon.* **16**, 79 (2022).
- [49] Ned Bowden, Scott Brittain, Anthony G. Evans, John W. Hutchinson, George M. Whitesides, Spontaneous formation of ordered structures in thin films of metals supported on an elastomeric polymer, *Nature* **393**, 146 (1998).
- [50] L. Mahadevan, S. Rica, Self-Organized Origami, *Science* **307**, 1740 (2005).
- [51] Dayong Chen, Jinhwan Yoon, Dinesh Chandra, Alfred J. Crosby, Ryan C. Hayward, Stimuli-Responsive Buckling Mechanics of Polymer Films, *J. Polym. Sci., Part B: Polym. Phys.* **52**, 1441 (2014).
- [52] Wenzhong Bao, Feng Miao, Zhen Chen, Hang Zhang, Wanyoung Jang, Chris Dames, Chun Ning Lau, Controlled ripple texturing of suspended graphene and ultrathin graphite membranes, *Nat. Nanotechnol.* **4**, 562 (2009).
- [53] Shikai Deng, Vikas Berry, Wrinkled, rippled and crumpled graphene: an overview of formation mechanism, electronic properties, and applications, *Mater. Today* **19**, 197 (2016).
- [54] Nestor Iguñiz, Riccardo Frisenda, Rudolf Bratschitsch, Andres Castellanos-Gomez, Revisiting the Buckling Metrology Method to Determine the Young's Modulus of 2D Materials, *Adv. Mater.* **31**, 1807150 (2019).
- [55] Quoc Huy Thi, Lok Wing Wong, Haijun Liu, Chun-Sing

- Lee, Jiong Zhao, Thuc Hue Ly, Spontaneously Ordered Hierarchical Two-Dimensional Wrinkle Patterns in Two-Dimensional Materials, *Nano Lett.* **20**, 8420 (2020).
- [56] Pablo Ares, Yi Bo Wang, Colin R. Woods, James Dougherty, Laura Fumagalli, Francisco Guinea, Benny Davidovitch, Kostya S. Novoselov, Van der Waals interaction affects wrinkle formation in two-dimensional materials, *Proc. Natl. Acad. Sci.* **118**, e2025870118 (2021).
- [57] Anikeya Aditya, Ankit Mishra, Nitish Baradwaj, Ken-ichi Nomura, Aiichiro Nakano, Priya Vashishta, Rajiv K. Kalia, Wrinkles, Ridges, Miura-Ori, and Moiré Patterns in MoSe₂ Using Neural Networks, *J. Phys. Chem. Lett.* **14**, 1732 (2023).